

## Temperature Dependence of Surface Segregation in Miscible Polymer Blend of Poly(4-trimethylsilylstyrene)/Polyisoprene

Daisuke KAWAGUCHI,<sup>1</sup> Masayuki OHYA,<sup>1</sup> Naoya TORIKAI,<sup>2</sup>  
Atsushi TAKANO,<sup>1</sup> and Yushu MATSUSHITA<sup>1,†</sup>

<sup>1</sup>*Department of Applied Chemistry, Graduate School of Engineering, Nagoya University,  
Furo-cho, Chikusa-ku, Nagoya 464-8603, Japan*

<sup>2</sup>*Neutron Science Laboratory, High Energy Accelerator Research Organization, 1-1 Oho, Tsukuba 305-0801, Japan*

(Received June 25, 2007; Accepted August 17, 2007; Published November 2, 2007)

**ABSTRACT:** Surface segregation behavior in miscible polymer blend thin film of poly(4-trimethylsilylstyrene)(PT)/polyisoprene (PI) was investigated as a function of temperatures on the basis of contact angle and neutron reflectivity measurements. For all temperatures employed, PT, which is a lower surface free energy component, is segregated at the surface of the blend film due to the requirement for minimizing the total free energy of the system. A concentration profile near the blend film surface is in good agreement with the mean-field prediction at 373 K and 393 K, being much lower than the lower critical solution temperature (LCST) for the blend in bulk. It was confirmed that decay length,  $\xi$ , and surface excess amount,  $z^*$ , increase with increasing temperature. On the other hand, a concentration fluctuation in the internal region becomes remarkable at 453 K, even below the LCST in bulk. Thus, it is concluded that a concentration fluctuation in PT/PI blend thin film below the LCST is induced by the surface segregation of PT component in blend thin film. [doi:10.1295/polymj.PJ2007089]

**KEY WORDS** Surface Segregation / Neutron Reflectivity / Poly(4-trimethylsilylstyrene) / Phase Separation / Thin Film /

Controlling surface and interfacial structures of soft materials is important to many applications such as coating, wetting, adhesion, and lubrication etc. Many researchers have investigated surface segregation phenomena in miscible polymer blends theoretically and experimentally.<sup>1–13</sup> In miscible mixtures of two polymers having equivalent degree of polymerization, a lower surface energy component is known to be enriched at surface due to the requirement for minimization of the total free energy of the system. The concentration profile near the surface for such mixtures can be well expressed by mean-field and self-consistent mean-field models.<sup>1–7</sup> This can be understood by taking into account thermodynamics at the surface.

In general, a rubbery component is segregated at the surface from glassy/rubbery polymeric blends at room temperature. It is well recognized that polystyrene (PS)/poly(vinyl methyl ether) (PVME) blend is the typical example in which the rubbery component, PVME, is preferentially segregated at the surface<sup>14–20</sup> even though both components are miscible each other in bulk.<sup>21–23</sup> Since a rubbery component possesses a lower density and/or a larger entropy, the surface free energy is relatively low in comparison with the glassy

component unless any other enthalpic interactions. In reality, to our knowledge, no reports are known for the glassy/rubbery blends in which the glassy component is segregated at the surface.

We have already found that poly(4-trimethylsilylstyrene) (PT), which is a glassy polymer as one of the PS derivatives, and polyisoprene (PI) with dominant 1,2- and 3,4-microstructures form a miscible polymer blend though PS and PI are a typical immiscible polymer blend.<sup>24</sup> Based on the small angle neutron scattering measurement and microscopic observation, it has been confirmed that the PT/PI blend exhibits a lower critical solution temperature (LCST) type phase diagram and is miscible at room temperature. These results indicate that miscibility of the blends can be drastically changed by introducing trimethylsilyl (TMS) groups into phenyl rings of PS. Thus, from the viewpoint of surface chemistry, PT is totally different from PS owing to hydrophobic and bulky TMS groups, therefore, a glassy component of PT may be enriched at the surface of PT/PI blend film. In fact, we have observed surface enrichment of PT component in an interdiffusion experiment of PT/PI bilayer films for a sufficiently long time,<sup>25</sup> though,

<sup>†</sup>To whom correspondence should be addressed (Tel:+81-52-789-4604, Fax:+81-52-789-3210, E-mail: yushu@apchem.nagoya-u.ac.jp).

surface state of PT/PI blend has not been systematically clarified yet. Moreover, surface segregation phenomena are dependent on temperature, composition and molecular weight. There are many studies for composition and molecular weight dependence of surface segregation phenomena in polymer blends, however, few works have been reported for the temperature dependence.

In this study, therefore, we focus on temperature dependence of surface segregation phenomena in PT/PI blend films. The concentration profiles near the blend film surfaces are investigated by *in situ* neutron reflectivity (NR) measurements and these are compared with the mean-field prediction.

## EXPERIMENTAL

Poly(4-trimethylsilylstyrene), hPT, its partially deuterated polymer, dPT, polyisoprene, PI, were used in this study. Figure 1 shows the chemical structures of hPT, dPT, and PI. All polymers were synthesized by anionic living polymerizations and the details of the syntheses of hPT and dPT were reported elsewhere.<sup>24–26</sup> Table I shows the characteristics of the samples used in this study. The weight average molecular weights,  $M_w$ s, were evaluated by multi angle laser light scattering (MALLS), DAWN EOS enhanced optical system of Wyatt Technology at

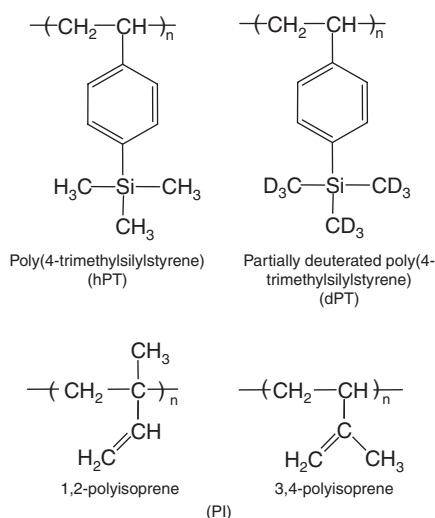


**Figure 1.** Chemical structures of poly(4-trimethylsilylstyrene) (hPT), partially deuterated poly(4-trimethylsilylstyrene) (dPT), 1,2-polyisoprene and 3,4-polyisoprene.

**Table I.** Characteristics of polymers used in this study

Sample	$M_w$	$M_w/M_n$	$T_g/K$
dPT	43 K	1.07	403
hPT	34 K	1.01	406
PI	11 K	1.07	283

308 K. The molecular weight distribution,  $M_w/M_n$ , was evaluated by gel permeation chromatography (GPC) using HLC-8020 of Tosoh Corp, where  $M_n$  denotes a number-average molecular weight. Glass transition temperatures,  $T_g$ s, were measured by differential scanning calorimetry under dry nitrogen purge at the heating rate of 10 K/min.

PT and PI homopolymers and their blend films were prepared by a spin-coating method from toluene solutions onto Si wafers with native oxide layer. Volume fraction of dPT used for neutron reflectivity measurements was set to be 0.5. The film thicknesses evaluated by X-ray reflectivity measurements were *ca.* 120 ~ 150 nm. Critical temperature,  $T_c$ , for this blend thin film was confirmed to be 444 K by optical microscopic measurements. The films were annealed at various temperatures for 120 h, the temperatures adopted are well above the  $T_g$  of the blend, 308 K, but below the LCST.

Surface free energies of PT, PI and their blend in thin film state were examined by contact angle measurement using Dropmaster 300 (Kyowa Interface Science Co., Ltd.). Water and diiodemethane were used as probe liquids. NR measurements were carried out using the reflectometer, Advanced Reflectivity for Interface and Surface Analysis (ARISA),<sup>27</sup> at Neutron Science Laboratory, High Energy Accelerator Research Organization in Tsukuba. Samples were heated in a vacuum cell at the various temperatures. Data were acquired in a setting temperature at fixed incident angles of *ca.* 0.25° and 0.60°. The wavelength range was from 0.12 to 0.70 nm, resulting in a scattering vector,  $q = (4\pi/\lambda) \sin \theta$ , range of 0.08–1.1 nm<sup>-1</sup>, where  $\lambda$  is the wavelength of neutrons and  $2\theta$  is the scattering angle. Angular resolution was set to be 5.0%. The reflectivity was calculated using the scattering length density, ( $b/V$ ), profile along depth direction by Parratt 32.<sup>28</sup>

## RESULTS AND DISCUSSION

### Surface Free Energy of the Homopolymers

Table II shows contact angles against water and diiodemethane and the corresponding surface free energies for dPT, hPT, PI and PS films calculated using Owens' method.<sup>29</sup> The total surface free energy,  $\gamma$ ,

**Table II.** Surface free energies of polymers used in this study

Sample	$\theta_{H_2O}/deg.$	$\theta_{CH_2I_2}/deg.$	Surface free energy/mJ m <sup>-2</sup>		
			$\gamma^d$	$\gamma^h$	$\gamma$
dPT	103.4	56.3	31.0	0.1	31.1
hPT	103.6	54.6	32.2	0.0	32.2
PI	102.4	45.1	38.0	0.0	38.0
PS	87.3	32.3	42.2	1.1	43.3

is expressed as the sum of two terms, *i.e.*,  $\gamma^h + \gamma^d$ , where  $\gamma^h$  and  $\gamma^d$  denote the components of surface free energy due to hydrogen bonding and dispersion force, respectively.  $\gamma$  of dPT and hPT are 31.1 and 32.2 mJ·m<sup>-2</sup>, respectively, and they are significantly lower than that of PS, 43.3 mJ·m<sup>-2</sup>, meaning that TMS groups contribute to an anomalous depression of  $\gamma$  for PT. According to Clarson's work in which surface composition of TMS terminated poly(methylphenylsiloxane) (PMPS)-PS diblock copolymer was investigated using time-of-flight secondary ion mass spectrometry (ToFSIMS),<sup>30</sup> the surfaces of the diblock copolymer films show an enrichment of TMS groups on chain ends. Furthermore, the prediction based on the group contribution method suggests that the  $\gamma$  of TMS group is much smaller than that of main chain.<sup>31</sup> Hence, it is reasonable to consider that the lower  $\gamma$  for PT in comparison with that for PS is caused by preferential orientation of TMS groups on phenyl rings at the surface for the former.

#### Composition Dependence of Surface Free Energy of the Blend Film

PT composition,  $\phi_{PT}$ , dependence of  $\gamma$  for PT/PI blend films was examined by contact angle measurements as shown in Figure 2.  $\gamma$  gradually decreases with decreasing  $\phi_{PT}$  in its range from 1.0 to 0.3, however, it steeply turns around at 0.1. The observed values of  $\gamma$  in the  $\phi_{PT}$  range from 1.0 to 0.3 are apparently lower than that of pure PT. This result implies that the hydrophobic TMS groups on PT in the blends are more oriented toward the surface with decreasing  $\phi_{PT}$ . Namely, it is expected that the PT molecule tends to possess a flattened conformation normal to the surface, resulting in losing a conformational entropy which may overcome an enthalpic gain. To discuss this phenomenon, chain conformation and orientation of TMS groups at the surface of PT/PI blend film in the small  $\phi_{PT}$  region will be investigated by NR and in conjunction with sum frequency generation and be reported in a separate work.<sup>32</sup>

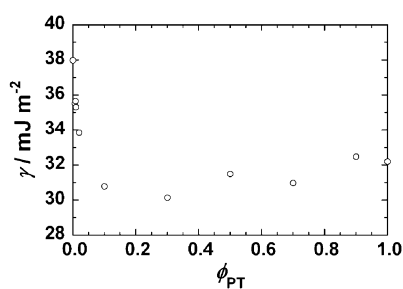


**Figure 2.** Composition dependence of surface free energies,  $\gamma$ , for PT/PI blends.  $\gamma$  values were calculated using Owens' equation on the basis of contact angles against water and diiodomethane.

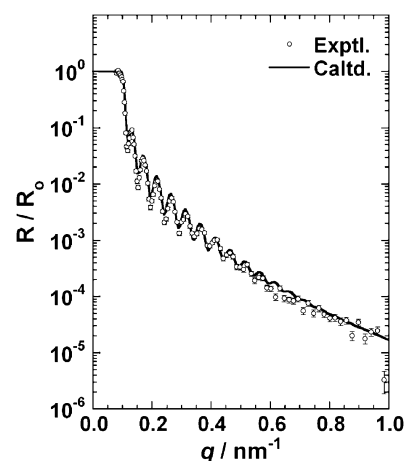


**Figure 3.** Scattering vector,  $q$ , dependence of neutron reflectivities for dPT/PI blend film annealed at 393 K. Experimental data set is shown by circles, and the best-fit curve calculated from the model scattering length density profile is expressed by the solid line.

#### Concentration Profile of PT/PI Blend Film

We evaluated concentration profiles of PT/PI blend films with  $\phi_{PT}$  of 0.5 as a function of temperature. In general, X-ray photoelectron spectroscopy (XPS) is a powerful tool to investigate the composition profile near film surfaces, however, the method could not be applied to the present blend film because the two polymer species are composed of neutral carbons and silicon, and the ratio of silicon to carbon is quite low. Therefore, in order to clarify the concentration profile near the surface, NR measurements were carried out, so that dPT was used as a blend component instead of hPT. Figure 3 shows the scattering vector,  $q$ , dependence of NR for the dPT/PI blend film annealed at 393 K. Experimental data set is represented by circles, while a solid curve denotes the best-fit calculated reflectivity to the experimental data based on the model scattering length density,  $(b/V)$ , profile, as shown in Figure 4(a). Since the calculated curve is in good accordance with the experimental data, it can be conceived that the model  $(b/V)$  profile well represents the composition profile in the film along normal to the surface. The calculated  $(b/V)$  values for dPT and PI are  $3.63 \times 10^{-4}$  and  $0.27 \times 10^{-4}$  nm<sup>-2</sup>, respectively, using the scattering lengths per monomeric units and bulk densities of these polymers.<sup>24</sup> A spike of  $(b/V)$  at around 125 nm in Figure 4(a) reflects the presence of a native oxide layer of the silicon wafer. The  $(b/V)$  value at the surface is nearly equal to that of pure dPT, meaning that dPT was preferentially segregated at the surface. On the other hand, the  $(b/V)$  value of approximately  $1.0 \times 10^{-6}$  nm<sup>-2</sup> in the substrate interfacial region is lower than that in bulk region, indicating that PI is preferentially segregated at the substrate interface. Thus, it is

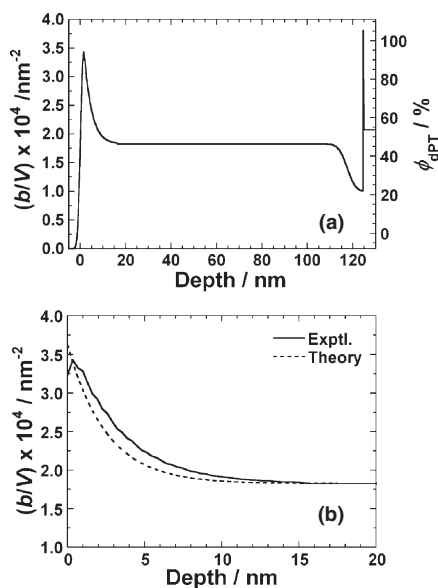


**Figure 4.** (a) Model scattering length density,  $(b/V)$ , profile for dPT/PI blend film annealed at 393 K. (b) Enlarged  $(b/V)$  profile near the blend film surface. Solid and dashed lines denote the experimentally measured profile and the predicted one using mean-field approximation.

evident that lower and higher surface energy components were segregated at the surface and interface, respectively, to minimize total free energy.

We now turn to a comparison of our data with the prediction by a mean-field approximation. According to Schmidt and Binder, the concentration profile of symmetric polymer blend film near surface can be approximated by eq 1.<sup>1</sup>

$$\phi(z) = \phi_{\infty} + (\phi_s - \phi_{\infty}) \exp\left(\frac{-z}{\xi}\right) \quad (1)$$

where  $\phi_s$  and  $\phi_{\infty}$  denote surface ( $z = 0$ ) and bulk volume fraction of dPT component, respectively, and  $\xi$  is the decay length showing how the surface composition reaches the bulk value.<sup>6</sup> Here,  $\phi_s$  is assumed to be unity at the top surface based on the experimental  $(b/V)$  profiles. Figure 4(b) compares the enlarged  $(b/V)$  profile near the blend film surface used for NR fitting and the calculated one following the mean-field theory. Solid and dashed lines express the experimentally measured  $(b/V)$  profile and the mean-field prediction. The experimental  $(b/V)$  profile is basically in good agreement with the predicted one but the former is slightly deviated from the exponential functional form predicted by the mean-field theory and is flattened near the surface. This phenomenon has been observed in other blend film surfaces,<sup>8</sup> however, explicit reasons for this phenomenon have not been clarified. There may be three reasons; one is the influence of surface confinement on local chain conformation of dPT and another is strong segregation of hy-

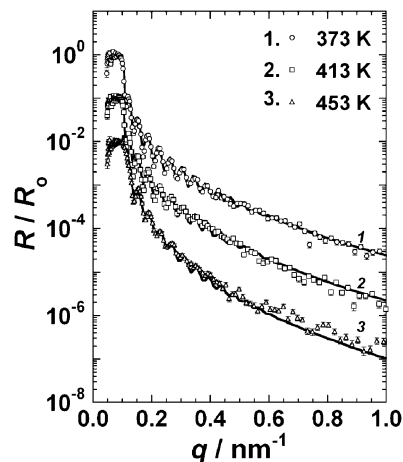


**Figure 5.**  $q$  dependence of neutron reflectivities for dPT/PI blend films as a function of annealing temperatures. Open circles, squares and triangles denote experimental NR for dPT/PI blend film annealed at 373 K, 413 K and 453 K, respectively. Solid curves denote the best-fit calculated NR based on model  $(b/V)$  profiles as shown in Figure 6. For the sake of clarity, NR curves are vertically offset.

drophobic TMS groups on phenyl rings whose  $(b/V)$  value is higher than the other chemical groups due to deuteriums, and the other is the effect of the roughness of the film surfaces. The root-mean-square roughness of the film is evaluated to be 0.6 nm based on the atomic force microscopic observation. This means that  $\phi_{\text{dPT}}$  near the top surface ( $z = 0$ ) is less than unity. All the factors would not be independent but related to each other. However, for the moment, it is hard to conclude which is the dominant factor.

#### Temperature Dependence of Surface Segregation in dPT/PI Blend

Figure 5 shows  $q$  dependence of NR for dPT/PI blend films as a function of annealing temperatures. Solid curves denote the best-fit calculated reflectivity to the experimental data based on the model  $(b/V)$  profiles as shown in Figure 6. At 373 K and 413 K, dPT and PI were enriched at the surface and the substrate interface, respectively, whereas the internal bulk region was regarded as a miscible homogeneous region. Such a concentration profile is qualitatively in good agreement with the one at 393 K as shown in Figure 4(a). On the other hand, the concentration profile at 453 K in bulk region was not homogeneous but fluctuated while dPT and PI were somewhat weakly segregated at the surface and the substrate interface in the similar manner as at 413 K. This phenomenon was also observed at 433 K though the data was not shown. These results indicate that the blend films approach the critical point of phase separation.

Flory-Huggins interaction parameter,  $\chi$ , between dPT and PI was previously evaluated to be  $\chi =$

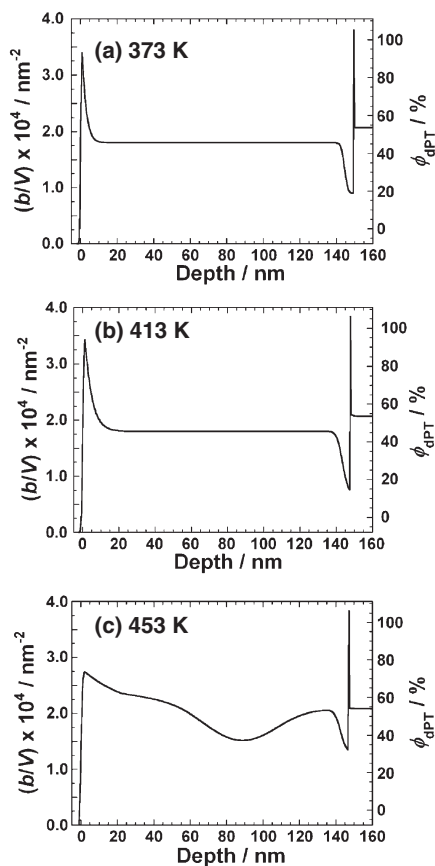


**Figure 6.** Model  $(b/V)$  profiles for dPT/PI blend films annealed at (a) 373 K, (b) 413 K and (c) 453 K.

$0.027 - 9.5/T$  based on small-angle neutron scattering.<sup>24</sup> Hence,  $\chi N$  value at 453 K can be calculated to be 1.16, where  $N (= 193)$  is a geometric mean of degree of polymerization for the two components. This estimated value is apparently lower than the critical one of 2. This means that the phase separation is liable to happen in thin film state. In fact, Tanaka *et al.* reported that the cloud point of PS/poly(vinyl methyl ether)(PVME) blend thin film decreased with decreasing film thickness.<sup>18</sup> Reich and Cohen explained that a decrease of the cloud point for PS/PVME thin film with decreasing thickness resulted from the selective adsorption of the PS segments on the hydrophilic substrate.<sup>33</sup> These results are similar to our present results for dPT/PI blend. Thus, it is obvious that the critical temperature of phase separation for dPT/PI blend thin film decreased in comparison with that in bulk.

To discuss the present results quantitatively, decay length,  $\xi$ , was analyzed based on  $(b/V)$  profiles.  $\xi$  values were deduced from the concentration profiles using eq. 1. Figure 7(a) displays the temperature dependence of  $\xi$  for dPT/PI blend films.  $\xi$  value at 373 K is nearly equivalent to that at 393 K, but its value increases with increasing temperature. Based on the mean-field theory,  $\xi$  should be equal to the corre-

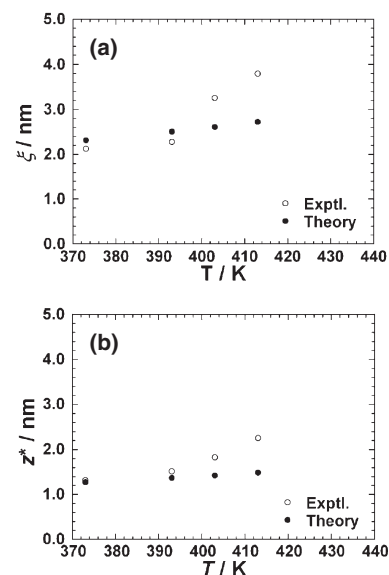


**Figure 7.** (a) Temperature dependence of  $\xi$  for dPT/PI blend films. Open circles represent  $\xi$  estimated based on  $(b/V)$  profiles and closed circles express the calculated  $\xi$  values using eq. 2. (b) Temperature dependence of  $z^*$  calculated based on the  $(b/V)$  profiles. Open and closed circles represent the experimental and theoretical values, respectively.

lation length for bulk concentration fluctuations and is given by;

$$\xi = \frac{a}{6} \left/ \left( \frac{1 - \phi_{\infty}}{2N_A} + \frac{\phi_{\infty}}{2N_B} - \chi\phi_{\infty}(1 - \phi_{\infty}) \right)^{1/2} \right. \quad (2)$$

where  $a$  is the statistical segment length,  $\chi$  is the Flory-Huggins interaction parameter,  $N_A$  and  $N_B$  are the degrees of polymerization for polymer species A and B.<sup>6</sup> For the blend films,  $a$  was estimated to be 0.66 nm, which is the averaged value for dPT, 0.72 nm, and PI, 0.60 nm.<sup>24,26</sup> The calculated  $\xi$  is represented by closed circles in Figure 7(a), where experimental values are in consistent with the theoretical ones at 373 K and 393 K, however, the formers start deviating from the theoretical ones at 403 K. This means that the blend film becomes more unstable with increasing temperature than expected by the theory, which is induced by surface and interfacial segregation which must be enhanced by the thin film effect.

Surface excess amount,  $z^*$ , was also evaluated.  $z^*$  is defined using  $\phi(z)$  as follows;

$$z^* = \int [\phi(z) - \phi_{\infty}] dz \quad (3)$$

where  $\phi_{\infty}$  is bulk volume fraction. The experimental  $z^*$  values were calculated from concentration profiles in Figure 6. On the other hand, the theoretical  $z^*$  value can be estimated from mean-field theory as well. According to Schmidt and Binder, the concentration profile near the surface can be expressed by eq. 1.<sup>1</sup> Hence, the  $\phi_s$  and  $\xi$  values for the current blend

system should be calculated. For a symmetric miscible blend,  $\phi_s$  can be estimated from

$$\phi_s = \frac{\phi_\infty + t}{1 + t} \quad (4)$$

where  $t$  is a parameter related to surface energy difference between the components,  $\Delta\gamma$ , and to Flory-Huggins interaction parameter,  $\chi$ . Here,  $t$  is given by

$$t = \left( \frac{3b^3 \Delta\gamma}{ak_B T} \right)^2 \frac{1}{\Delta\chi} \quad (5)$$

where  $b^3$  is volume of a Flory-Huggins lattice site,  $a$  is statistical segment length,  $k_B$  is Boltzmann constant,  $T$  is absolute temperature, and  $\Delta\chi = \chi_b - \chi$ . For the blends, the  $b^3$  values were taken to be averaged for dPT and PI:  $b^3_{\text{dPT}} = 3.05 \times 10^{-1} \text{ nm}^3$ ,  $b^3_{\text{PI}} = 1.22 \times 10^{-1} \text{ nm}^3$ . And,  $\Delta\gamma$  is  $6.9 \text{ mJ m}^{-2}$ . Also,  $\chi_b$  was introduced by Jones and Kramer as  $\chi$  on the coexistence curve, which can be given by the expression,<sup>6</sup>

$$\chi_b = \frac{1}{N(1 - 2\phi_\infty)} \ln \left( \frac{1 - \phi_\infty}{\phi_\infty} \right) \quad (6)$$

Figure 7(b) shows temperature dependence of  $z^*$  for dPT/PI blend films. Open and closed circles represent experimental and theoretical values. The theoretical  $z^*$  was calculated from eqs. 1–6. From Figure 7(b), we notice that the experimental values of  $z^*$  deviate from the theoretical ones with increasing temperature, whose tendency is similar to that for  $\xi$ . Thus, it is concluded that the surface enrichment of dPT component is enhanced, successively, phase separation is induced in the dPT/PI blend film with an increase of temperature.

## CONCLUSIONS

$\gamma$  of PT was examined by contact angle measurement and it was confirmed to be much lower than that of PS, meaning that hydrophobic TMS groups are segregated at and covered the surface in PT film. For all temperatures employed, PT, which is a lower surface free energy component, is segregated at the surface of the blend film due to the requirement for minimizing the total free energy of the system. A concentration profile near the blend film surface was in good agreement with the mean-field prediction at 393 K, being much lower than the LCST for the blend in bulk. It was confirmed that  $\xi$  and  $z^*$  increase with increasing temperature. On the other hand, a concentration fluctuation in the internal region becomes remarkable at 453 K, even below the LCST in bulk. Thus, it is concluded that a concentration fluctuation in PT/PI blend thin film below the LCST is induced by the surface segregation of PT component in blend thin film.

**Acknowledgment.** This work was in part supported by Grant-in-Aids for Scientific Research on Priority Area “Soft Matter Physics” and for Young Scientists B (No. 17750108) from the Ministry of Education, Culture, Sports, Science and Technology, Japan. This work was also partially supported by Inter-Univ. Program for common use KENS facility.

## REFERENCES

1. I. Schmidt and K. Binder, *J. Phys. (Paris)*, **46**, 1631 (1985).
2. R. A. L. Jones, E. J. Kramer, M. H. Rafailovich, J. Sokolov, and S. A. Schwarz, *Phys. Rev. Lett.*, **62**, 280 (1989).
3. R. A. L. Jones, L. J. Norton, E. J. Kramer, R. J. Composto, R. S. Stein, T. P. Russell, A. Mansour, A. Karim, G. P. Felcher, M. H. Rafailovich, J. Sokolov, X. Zhao, and S. A. Schwarz, *Europhys. Lett.*, **12**, 41 (1990).
4. A. Hariharan, S. K. Kumar, and T. P. Russell, *Macromolecules*, **24**, 4909 (1991).
5. S. A. Schwarz, B. J. Wilkens, M. A. A. Pudensi, M. H. Rafailovich, J. Sokolov, X. Zhao, W. Zhao, X. Zheng, T. P. Russell, and R. A. L. Jones, *Mol. Phys.*, **76**, 937 (1992).
6. R. A. L. Jones and E. J. Kramer, *Polymer*, **34**, 115 (1993).
7. J. Genzer, A. Faldi, and R. J. Composto, *Phys. Rev. E*, **50**, 2373 (1994).
8. L. J. Norton, E. J. Kramer, F. S. Bates, M. D. Gehlsen, R. A. L. Jones, A. Karim, G. P. Felcher, and R. Kleb, *Macromolecules*, **28**, 8621 (1995).
9. J. Genzer, A. Faldi, R. Oslanec, and R. J. Composto, *Macromolecules*, **29**, 5438 (1996).
10. K. Tanaka, T. Kajiyama, A. Takahara, and S. Tasaki, *Macromolecules*, **35**, 4702 (2002).
11. A. Opdahl, R. A. Phillips, and G. A. Somorjai, *Macromolecules*, **35**, 4387 (2002).
12. V. S. Minnikanti and L. A. Archer, *Macromolecules*, **39**, 7718 (2006).
13. D. Kawaguchi, K. Tanaka, N. Torikai, A. Takahara, and T. Kajiyama, *Langmuir*, **23**, 7269 (2007).
14. D. H. K. Pan and W. M. Prest, *J. Appl. Phys.*, **58**, 2861 (1985).
15. Q. S. Bhatia, D. H. Pan, and J. T. Koberstein, *Macromolecules*, **21**, 2166 (1988).
16. G. T. Dee and B. B. Sauer, *Macromolecules*, **26**, 2771 (1993).
17. J. M. G. Cowie, B. G. Devlin, and I. J. McEwen, *Macromolecules*, **26**, 5628 (1993).
18. K. Tanaka, J.-S. Yoon, A. Takahara, and T. Kajiyama, *Macromolecules*, **28**, 934 (1995).
19. D. Kawaguchi, K. Tanaka, T. Kajiyama, A. Takahara, and S. Tasaki, *Macromolecules*, **36**, 6824 (2003).
20. C. Forrey, J. T. Koberstein, and D. H. Pan, *Interface Sci.*, **11**, 211 (2003).
21. T. K. Kwei, T. Nishi, and R. F. Roberts, *Macromolecules*, **7**, 667 (1974).
22. T. Nishi and T. K. Kwei, *Polymer*, **16**, 285 (1975).
23. L. A. Utracki, in “Polymer Alloys and Blends, Thermodynamics and Rheology,” Carl Hanser Verlag, Munich, 1989.
24. M. Harada, T. Suzuki, M. Ohya, D. Kawaguchi, A. Takano, and Y. Matsushita, *Macromolecules*, **38**, 1868 (2005).

25. M. Harada, M. Harada, T. Suzuki, M. Ohya, D. Kawaguchi, A. Takano, Y. Matsushita, and N. Torikai, *J. Polym. Sci., Part B: Polym. Phys.* **43**, 1486 (2005).
26. M. Harada, T. Suzuki, M. Ohya, A. Takano, and Y. Matsushita, *Polym. J.*, **36**, 538 (2004).
27. N. Torikai, M. Furusaka, H. Matsuoka, Y. Matsushita, M. Shibayama, A. Takahara, M. Takeda, S. Tasaki, and H. Yamaoka, *Appl. Phys. A*, **74**, S264 (2002).
28. [http://www.hmi.de/bensc/instrumentation/instrumente/v6/refl/parratt\\_en.htm](http://www.hmi.de/bensc/instrumentation/instrumente/v6/refl/parratt_en.htm)
29. D. K. Owens and R. C. Wendt, *J. Appl. Polym. Sci.*, **13** 1741 (1969).
30. S. J. Clarson, J. O. Stuart, C. E. Selby, A. Sabata, S. D. Smith, and A. Ashraf, *Macromolecules*, **28**, 674 (1995).
31. C. Jalbert, J. T. Koberstein, A. Hariharan, and S. K. Kumar, *Macromolecules*, **30**, 4481 (1997).
32. D. Kawaguchi, L. Zhang, Y. Ouchi, M. Ohya, N. Torikai, A. Takano, and Y. Matsushita, manuscript in preparation.
33. S. Reich and Y. Cohen, *J. Polym. Sci., Polym. Phys. Ed.*, **19**, 1255 (1981).